Nuclear Measurements of Fuel–Shell Mix in Inertial Confinement Fusion Implosions on OMEGA

Introduction

Turbulent mix is a vital concern in inertial confinement fusion (ICF)[1,2] since it can quench the nuclear burn in the hot spot prematurely, or even extinguish it entirely. The saturation of Rayleigh–Taylor (RT) instability growth at a density interface leads to small-scale, turbulent eddies that in turn lead to mixing of the high- and low-density materials.[3] These mixing processes can disrupt the formation of the low-density hot spot, lowering its temperature and reducing its volume. The resulting lower nuclear production can fail to ignite the capsule. Understanding the extent of mix under different conditions is a crucial step toward mitigating its adverse effects.

A substantial and sustained effort to understand hydrodynamic instabilities and mix has been ongoing for many decades, due in large part to their heavy impact on ICF. Reviews of the literature on experimental, computational, and theoretical work on hydrodynamic instabilities and mix can be found on, for example, the first page of Refs. 4 and 5. Related work on mix in ICF implosions includes papers by Li,[6] Radha,[7] Regan,[8] and Wilson,[9] as well as many others.

This article reviews and extends aspects of the work published by Li *et al*.[6] over a wider range of capsule parameters. In addition, we calculate a quantitative upper limit on the null result published by Petrasso *et al*.[10] of the amount of mix at the time of shock collapse, which occurs before the onset of the deceleration phase. Results from time-dependent nuclear production history measurements of the mix region will be published elsewhere.[11] A brief review of the causes and effects of mix can be found in the next section. The remaining sections (1) describe the experimental setup, (2) present experimental observations, (3) describe the constraint on the amount of fuel–shell mix between shock collapse and deceleration-phase onset, and (4) summarize our results.

Causes and Effects of Mix

When a fluid of density ρ_1 accelerates a heavier fluid of density ρ_2, the fluid interface is RT unstable. The rapid growth of initial perturbations sends spikes of the heavy fluid into the light fluid, while bubbles of the light fluid penetrate into the heavy fluid. The exponential growth eventually saturates into a nonlinear regime where the spike and bubble amplitudes grow quadratically in time. As the spikes and bubbles continue to interpenetrate, velocity shear between the two fluids results in further instability (the drag-driven Kelvin–Helmholtz instability), causing the spike tips to "mushroom" and roll up on increasingly finer scales, increasing the vorticity of the flow and eventually leading to mixing of the two fluids on the atomic scale.

In ICF, both the acceleration and deceleration phases have RT-unstable surfaces.[2] The low-density ablating mass pushes against the high-density "payload" during the acceleration phase, and after further convergence and compression, the high-density shell is stopped by the low-density hot spot during the deceleration phase. Initial perturbations are seeded by laser and target surface nonuniformities, and growth of these perturbations during the acceleration phase can feed through to the inner surface and contribute to seeding perturbations for the deceleration phase.[2]

Unmitigated RT growth during the acceleration phase can eventually break through the shell, compromising its compressibility and reducing the attainable areal density of the assembled target at stagnation. RT growth during the deceleration phase can send spikes of cold, dense fuel into the central hot spot, potentially disrupting its formation. Even if the spikes do not reach the center, their penetration and the resultant mixing of the cold, dense shell with the low-density hot spot will cool the outer regions of the hot spot, reducing the volume participating in nuclear production.

Experimental Setup

Direct-drive implosions were conducted on OMEGA,[12] with 60 beams of frequency-tripled (351 nm) UV light in a 1-ns square pulse and a total energy of 23 kJ. One-THz-bandwidth smoothing by spectral dispersion and polarization smoothing of the laser beam were used.[13] The beam-to-beam energy imbalance was typically between 2% and 4% rms. The spherical capsules had diameters between 860 and 940 μm, plastic-shell thicknesses of 20, 24, or 27 μm, and a surface coating of 0.1 μm of aluminum.

Three target configurations were used (Fig. 109.14): The reference "CH" capsules had shells made of plastic (CH) and a gaseous fill of D_2 and ^{3}He. "CD" capsules had gaseous fills of pure ^{3}He, and a shell made mostly of CH, except for a 1-μm layer of deuterated plastic (CD) on the inner surface. "CD offset" capsules are like the CD capsules, except that the 1-μm CD layer is offset from the inner surface by 1 μm of CH. The composition of the ordinary plastic consists of an H to C ratio of 1.38, and the deuterated plastic has a D to C ratio of 1.56 (Ref. 6).
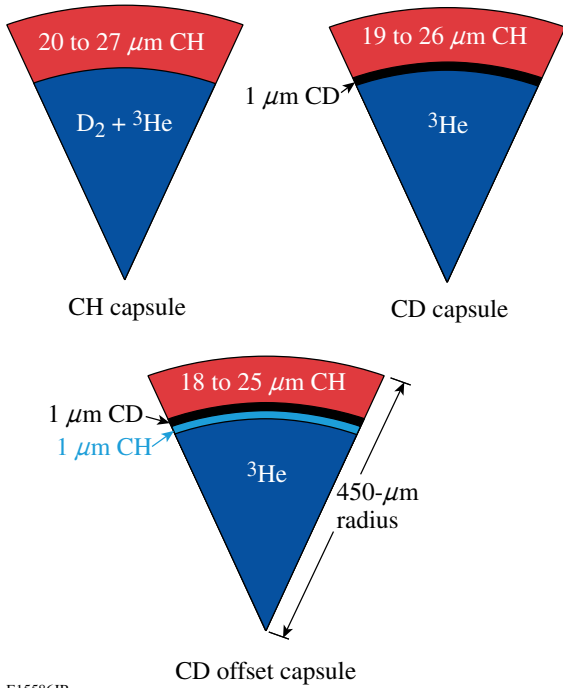
Figure 109.14
0.5 or 2.5 mg/cm^3 of pure ^{3}He gas fills a 20- to 27-μm-thick plastic shell with a 1-μm deuterated layer either adjacent to the inner surface (CD capsule) or offset from the inner surface by 1 μm (CD offset capsule). The reference (CH capsule) contains D^{3}He gas and has no deuterated layer. Whereas CH capsules will produce D^{3}He protons whenever the fuel gets sufficiently hot, CD capsules will produce only D^{3}He protons if the fuel and shell become atomically mixed.

The pure ^{3}He gases were filled to initial pressures of 4 and 20 atm at a temperature of 293 K, corresponding to initial mass densities (ρ_0) of 0.5 and 2.5 mg/cm^3. The D_2–^{3}He gas is an equimolar mixture of D to ^{3}He by atom and is filled to a hydro-dynamically equivalent initial pressure as the pure-^{3}He fill, as described in Ref. 14. Because fully ionized D and ^{3}He have the same value of $(1 + Z)/A$, mixtures with the same mass density will also have the same total particle density and equation of state and can be considered hydrodynamically equivalent. For

the 4- and 20-atm ^{3}He fills, the hydrodynamically equivalent D_2–^{3}He pressures are 3.6 and 18 atm, respectively.

Hydrodynamic simulations of capsule implosions using the 1-D code *LILAC*[15] showed only minor differences in the timing and profiles between the equivalent CH and CD implosions. The convergence ratio C_r, defined as the initial inner capsule radius over the fuel–shell interface radius at the time of stagnation, for capsules with different shell thicknesses and initial fill density is shown in Table 109.I.

Table 109.I: Predicted convergence ratio C_r calculated by *LILAC* for different capsule parameters. Capsules with higher convergence ratios are expected to be more susceptible to mix. The convergence ratio does not differ significantly between CH and CD capsules.

ρ_0 (mg/cm^3)	Thickness (μm)	C_r (1-D)
0.5	20	38.0
0.5	24	35.2
0.5	27	31.5
2.5	20	14.9
2.5	24	14.5
2.5	27	13.8

The following primary nuclear reactions can occur in targets containing both D_2 and ^{3}He:

$$D + D \rightarrow {}^3\text{He} + n(2.45 \text{ MeV}),$$
$$D + D \rightarrow T + p(3.0 \text{ MeV}), \quad (1)$$
$$D + {}^3\text{He} \rightarrow {}^4\text{He} + p(14.7 \text{ MeV}),$$
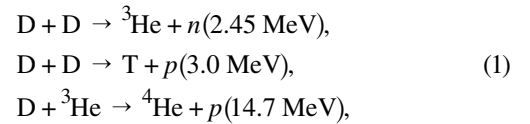
where the number in parentheses is the mean birth energy of the second product.

The set of capsules shown in Fig. 109.14 is ideal for studying the nature and extent of turbulent mix in ICF implosions. Whereas implosions of CH capsules will produce D^{3}He protons whenever the fuel gas gets sufficiently hot, heating alone is not sufficient for D^{3}He production in CD and CD offset capsules. To produce measurable D^{3}He yields, these capsules require in addition the mixing of the fuel and shell on an atomic scale. Measurement or absence of the D^{3}He yield in implosions of CD offset capsules can be used to ascertain the extent into the shell that turbulent mixing processes reach.

Fuel–shell mix is not a requirement to produce DD-n yields in CD and CD offset implosions, but measurement of the DD-n yield provides a useful way to determine if the CD layer was heated to temperatures near 1 keV.

The primary diagnostics for this study were wedged-range-filter (WRF) spectrometers,[16] to measure the D^3He proton yield and spectrum, and neutron time-of-flight (nTOF) scintillator detectors,[17] to measure the DD-n yield. On a given shot, up to six WRF spectrometers were used simultaneously to improve the estimate of the D^3He yield.[16] The D^3He proton spectrum measured from implosions of D^3He-filled CH capsules often shows two distinct components, corresponding to D^3He proton emission shortly after the collapse of the converging shock and to emission during the deceleration phase, about 300 ps later.[10,18]

Experimental Results

1. Yield Measurements

Turbulent mixing of the fuel and shell is demonstrated by measurements of finite D^3He yields (Y_p) in ^3He-filled, CD capsules (see Fig. 109.15 and Ref. 6). The shock component, apparent in the spectrum of the CH capsule implosion above 14 MeV, is absent in the CD capsule. All D^3He yields reported in this section for CH capsules will include only the compression component; the shock component will be considered in the following section.

The D^3He yields from CD capsules are at least two orders of magnitude higher than would be expected by the interaction of thermal ^3He ions penetrating through the CD layer surface,[6] even with enhanced surface area resulting from a RT-perturbed surface. The D^3He yields are at least three orders of magnitude higher than the maximum that would be expected if some ^3He had diffused into the CD layer between the times of fabrication and implosion.[6] For yields as high as have been observed, there must be a region that has been heated to at least 1 keV and where the fuel and shell have experienced atomic mix.

Significant D^3He yield from CD-offset implosions demonstrates that there is substantial mixing of the fuel with the "second" 1-μm layer of the shell (Fig. 109.16). Thermal ^3He ions cannot penetrate through the first micron of the shell to produce
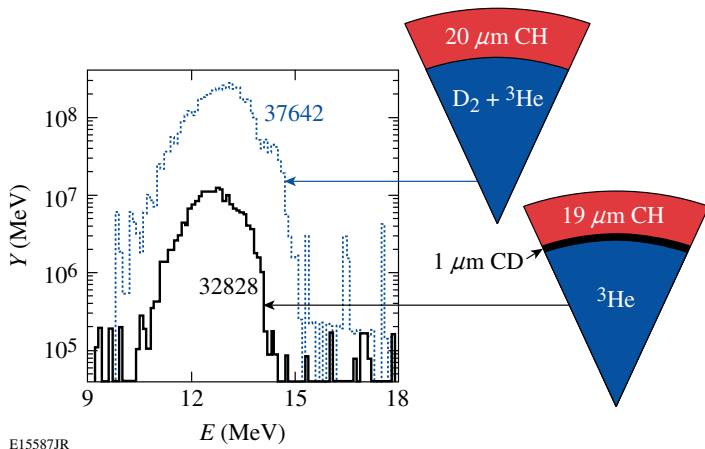
Figure 109.15
D^3He proton spectra from a CH capsule (shot 37642) and from a CD capsule (shot 32828) with 2.5-mg/cm^3 initial fill density. The high D^3He yield from CD implosions demonstrates the existence of fuel–shell mix. The CD implosion yield, although substantially less than the yield from the CH implosion, is much higher than what would be expected in the absence of turbulent fuel–shell mix.
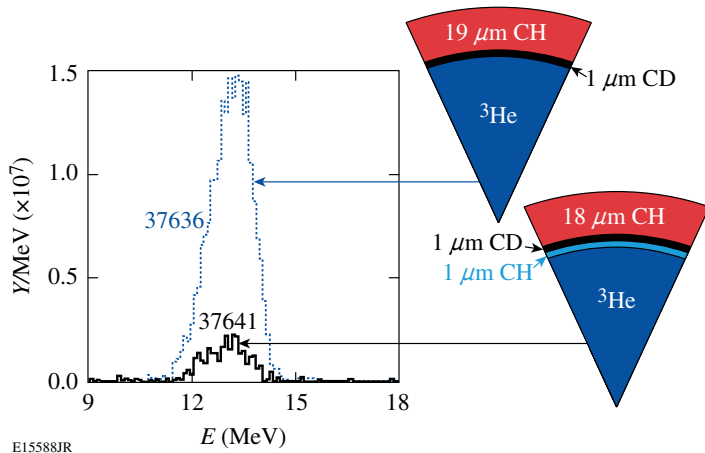
Figure 109.16
D^3He proton spectra from a CD capsule (shot 37636) and from a CD offset capsule (shot 37641) with 0.5-mg/cm^3 initial fill density. The D^3He yield drops by only a factor of 5 to 10 when the CD layer is offset from the inner surface by 1 μm, demonstrating that a substantial amount of the second micron of the shell is mixed with the fuel.

these yields, so the second micron must be exposed to the fuel by bubble growth and then mixed through turbulent processes.

The decreasing yields for increasing ρ_0 in CD capsules contrast strongly with the increasing yields for increasing initial ρ_0 in the reference CH capsules (see Fig. 109.17). This is evidence that the extent of mix is reduced for increasing initial fill density, since Y_p in CD implosions is lower, even though the core conditions are more favorable for nuclear production, as seen by the higher value of Y_p for CH implosions. Y_p in CD-offset implosions decreases by an additional factor of 5 and 10 compared to inner CD capsule implosions for 0.5 and 2.5 mg/cm^3 fills, respectively.

The lower DD-n yield (Y_n) for CD implosions with higher ρ_0 indicates that less heating of the CD layer occurred in these

implosions. Additional heating of the inner surface of the shell can occur through thermal conduction from and turbulent mix with the hot fuel. The lower Y_n supports the picture of reduced mix for higher-density fills.

Yields in both CH and CD implosions decrease with increasing shell thickness (Fig. 109.18). Thicker shells decrease Y_p by a larger factor in CD capsules compared to CH capsules, which suggests that the effects of mix are diminished. However, Y_n decreases by a smaller factor in CD capsules, which may be due to temperature effects dominating mix effects for the neutron yield in such implosions.

2. Areal Density Measurements
Evidence for a delay in nuclear production can be found through measurement of the compression of the target at bang time by

E15589JR
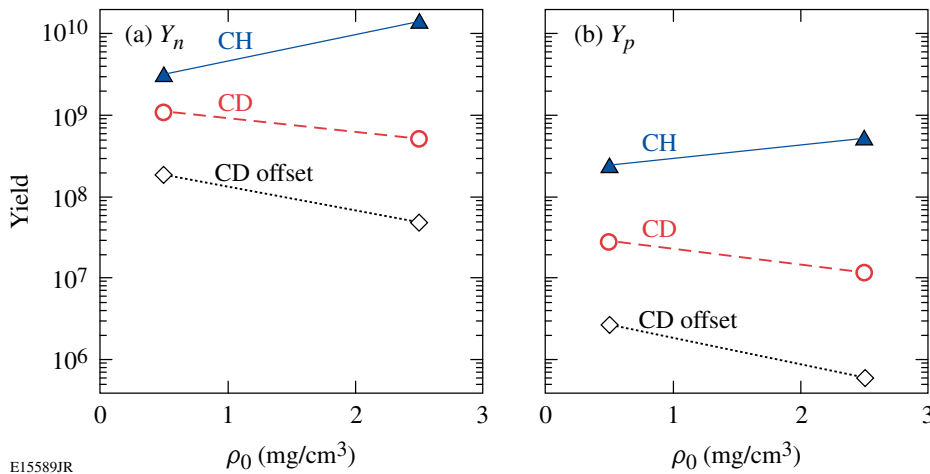
Figure 109.17
(a) DD-n and (b) D^{3}He yields from CH (solid triangles), CD (open circles), and CD-offset (open diamonds) implosions as a function of initial fill density for 20-μm-thick shells. Yields from CD and CD-offset implosions decrease with increasing fill density, in contrast to the increasing yields from CH implosions. Points show the mean of each shot ensemble, where the standard error in the mean is smaller than the size of the markers.

E15590JR
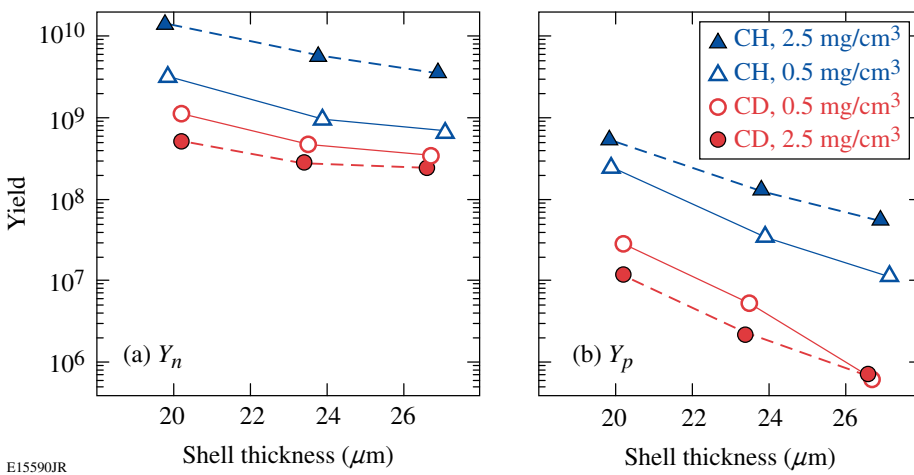
Figure 109.18
(a) DD-n and (b) D^{3}He yield in CH (triangles) and CD (circles) capsules with low (open markers) and high (solid markers) ρ_0 as a function of shell thickness. Capsules with lower ρ_0 are more susceptible to mix for all shell thicknesses.

means of the areal density ρR. Areal density is inferred from the mean downshift of the D^3He proton spectrum from the birth energy of 14.7 MeV, so the inferred ρR is an average measurement of ρR over the time of nuclear production. Because the capsule continues to compress, and ρR to increase, throughout the deceleration phase, one would expect that if bang time occurs during a later stage of the deceleration phase for an otherwise equivalent

implosion, then the average ρR would be higher.[11,18] As seen in Fig. 109.19, the inferred burn-averaged ρR is higher for implosions of CD capsules than for CH capsules. This is qualitatively consistent with the later bang times measured for CD capsules.

The experimental results of these experiments are summarized in Table 109.II. The mean and standard error are shown of
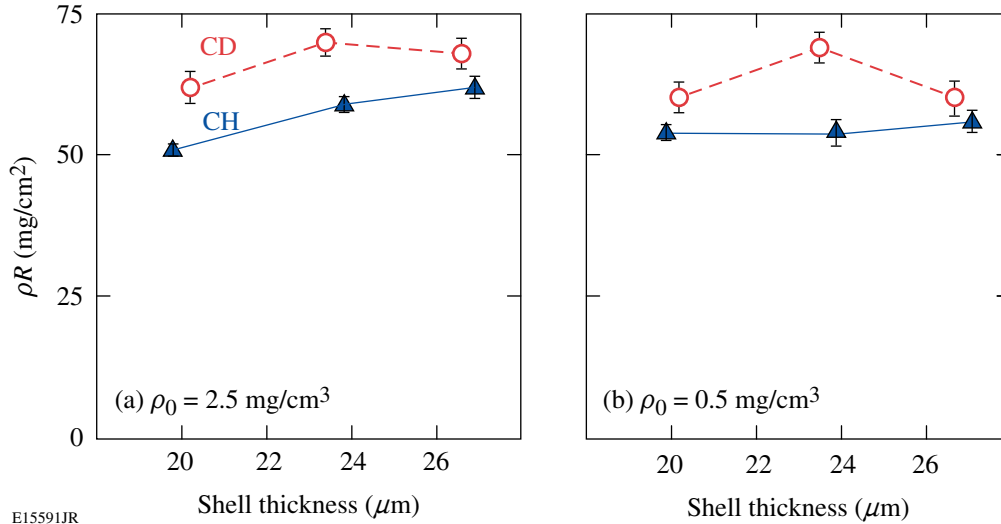
Figure 109.19
Mean and standard error of ρR's for CH (solid markers) and CD (open markers) implosions as a function of shell thickness with (a) high- and (b) low-density fills. The D^3He burn-averaged ρR is consistently higher for CD capsules.

E15591JR

Table 109.II: Experimental yield and areal density results of CH, CD, and CD-offset capsule implosions. The values shown are the mean and standard error of all shots in a particular ensemble, with the yield errors expressed as a percent of the mean. The quoted D^3He yield and areal density for CH capsules include the compression component only.

Type	ρ_0 (mg/cm^3)	Thickness (μm)	Number of shots	Y_n ($\times 10^8$)	Error (%)	Y_p ($\times 10^7$)	Error (%)	ρR (mg/cm^2)	Error
CH	0.5	19.9	17	31.3	6	24.3	11	54	1.5
CH	0.5	23.9	9	9.6	6	3.5	12	54	2.3
CH	0.5	27.1	8	6.7	7	1.13	30	56	2.0
CH	2.5	19.8	61	142	4	54.4	5	51	1.0
CH	2.5	23.8	26	58	5	13.2	8	59	1.3
CH	2.5	26.9	16	35	5	5.6	8	62	2.0
CD	0.5	20.2	7	10.8	10	2.9	10	60	2.4
CD	0.5	23.5	5	4.7	7	0.54	9	69	2.6
CD	0.5	26.7	2	3.4	7	0.06	7	60	3.1
CD	2.5	20.2	11	5.2	8	1.25	13	62	2.8
CD	2.5	23.4	7	2.7	15	0.22	19	70	2.4
CD	2.5	26.6	4	2.4	5	0.07	4	68	2.7
CD-off	0.5	19.2	3	1.9	17	0.28	28	52	1.7
CD-off	0.5	23.7	2	1.2	14	–	–	–	–
CD-off	2.5	18.4	5	0.5	24	0.06	14	55	3.0
CD-off	2.5	22.8	3	1.2	49	–	–	–	–

the DD-n and D^{3}He yields (Y_n and Y_p) and the areal density ρR inferred from the mean downshift of 14.7-MeV D^{3}He protons for CH, CD, and CD-offset capsules. Also shown is the number of shots of each kind. The mean is the average of measured values within a given shot ensemble, and the standard error is the standard deviation of the measurements divided by the square root of the number of shots.

Constraint on the Possibility of Mix During the Coasting Phase

Comparative analysis of D^{3}He-p spectra from CH and CD implosions can be used to place an upper bound on the possible amount of mix at shock time. For the representative spectrum of a CH capsule shown in Fig. 109.20, the total yield in the region from 14.2 to 14.7 MeV, corresponding to the shock component, is $1.7\pm0.2\times10^7$, or $3.7\pm0.3\%$ of the total yield. The yield in the same region of the representative spectrum from a CD capsule comes to $2.6\pm2.5\times10^4$, equal to $0.14\pm0.13\%$ of the total yield, and is consistent with zero.
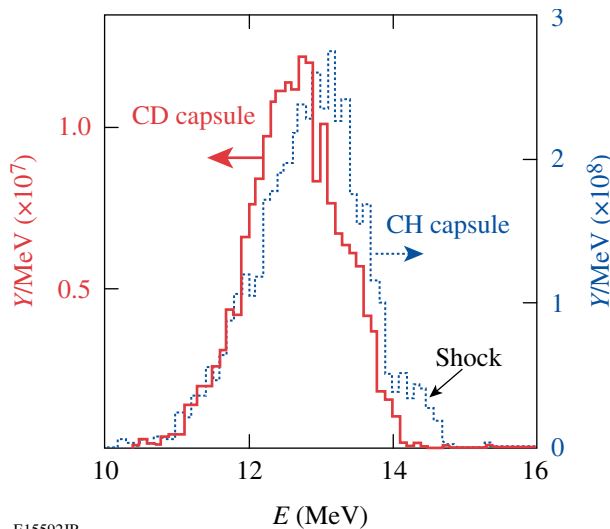
E15592JR

Figure 109.20
D^{3}He proton spectra from implosions of 20-μm-thick shells filled with 2.5 mg/cm^3 of fuel with CH (shot 37642, dotted) and CD (shot 32828, solid) shell configurations. The shock component of the CH implosions comes to 3.7% of the total yield, whereas the shock component contribution to the CD implosion spectrum is consistent with zero.

The "shock yield" of the CD implosion ($\leq 2.6\times10^4$) comes to, at most, 0.15% of the shock yield of the corresponding CH implosion (1.7×10^7). This yield ratio can be used to constrain the deuterium fraction by atom $f_D \leq 0.05\%$ in the fuel of the CD implosion during shock burn, by application of Eq. (5) in Ref. 14. Equation (5) assumes that f_D is uniform through the fuel region, so it does not preclude the more likely physical situation of deuterium concentrations higher than the above constraint in the outer, cooler region of the fuel.

Summary

The extent of fuel–shell mix has been shown to include a substantial amount of the shell from the inner first and second micron of the original material using ^{3}He-filled, CD-shell target implosions. The observed yields are higher than is consistent with diffusive mixing, so they must be the result of turbulent mixing down to the atomic scale.

The improved stability of capsules with higher initial fuel density and thicker initial shells has been confirmed by comparing the yield trends of CH, CD, and CD-offset capsules. Increasing the capsule fill density decreased the D^{3}He and DD-n yields for CD capsules and increased the yields for CH capsules, thereby demonstrating that the extent of mix is reduced for increasing initial fill density.

The D^{3}He shock yield in CD capsules with high initial fill density was constrained to be less than 0.14% of the total D^{3}He yield, and the average atomic fraction of deuterium in the fuel during the shock burn has been constrained to be less than 0.05% and is consistent with zero.

REFERENCES

1. J. Nuckolls *et al.*, Nature **239**, 139 (1972).

2. S. Atzeni and J. Meyer-ter-Vehn, *The Physics of Inertial Fusion: Beam Plasma Interaction, Hydrodynamics, Hot Dense Matter, International Series of Monographs on Physics* (Clarendon Press, Oxford, 2004).

3. P. E. Dimotakis, Annu. Rev. Fluid Mech. **37**, 329 (2005).

4. G. Dimonte, Phys. Plasmas **6**, 2009 (1999).

5. A. J. Scannapieco and B. Cheng, Phys. Lett. A **299**, 49 (2002).

6. C. K. Li, F. H. Séguin, J. A. Frenje, S. Kurebayashi, R. D. Petrasso, D. D. Meyerhofer, J. M. Soures, J. A. Delettrez, V. Yu. Glebov, P. B. Radha, F. J. Marshall, S. P. Regan, S. Roberts, T. C. Sangster, and C. Stoeckl, Phys. Rev. Lett. **89**, 165002 (2002).

7. P. B. Radha, J. Delettrez, R. Epstein, V. Yu. Glebov, R. Keck, R. L. McCrory, P. McKenty, D. D. Meyerhofer, F. Marshall, S. P. Regan, S. Roberts, T. C. Sangster, W. Seka, S. Skupsky, V. Smalyuk, C. Sorce, C. Stoeckl, J. Soures, R. P. J. Town, B. Yaakobi, J. Frenje, C. K. Li, R. Petrasso, F. Séguin, K. Fletcher, S. Padalino, C. Freeman, N. Izumi, R. Lerche, and T. W. Phillips, Phys. Plasmas **9**, 2208 (2002).

8. S. P. Regan, J. A. Delettrez, F. J. Marshall, J. M. Soures, V. A. Smalyuk, B. Yaakobi, V. Yu. Glebov, P. A. Jaanimagi, D. D. Meyerhofer, P. B. Radha, W. Seka, S. Skupsky, C. Stoeckl, R. P. J. Town, D. A. Haynes, Jr., I. E. Golovkin, C. F. Hooper, Jr., J. A. Frenje, C. K. Li, R. D. Petrasso, and F. H. Séguin, Phys. Rev. Lett. **89**, 085003 (2002).

9. D. C. Wilson, C. W. Cranfill, C. Christensen, R. A. Forster, R. R. Peterson, H. M. Hoffman, G. D. Pollak, C. K. Li, F. H. Séguin, J. A. Frenje, R. D. Petrasso, P. W. McKenty, F. J. Marshall, V. Yu. Glebov, C. Stoeckl, G. J. Schmid, N. Izumi, and P. Amendt, Phys. Plasmas **11**, 2723 (2004).

10. R. D. Petrasso, J. A. Frenje, C. K. Li, F. H. Séguin, J. R. Rygg, B. E. Schwartz, S. Kurebayashi, P. B. Radha, C. Stoeckl, J. M. Soures, J. Delettrez, V. Yu. Glebov, D. D. Meyerhofer, and T. C. Sangster, Phys. Rev. Lett. **90**, 095002 (2003).

11. J. R. Rygg, J. A. Frenje, C. K. Li, F. H. Séguin, R. D. Petrasso, V. Yu. Glebov, D. D. Meyerhofer, T. C. Sangster, and C. Stoeckl, "Time-Dependent Nuclear-Measurements of Fuel–Shell Mix in Inertial Confinement Fusion," submitted to Physical Review Letters.

12. T. R. Boehly, D. L. Brown, R. S. Craxton, R. L. Keck, J. P. Knauer, J. H. Kelly, T. J. Kessler, S. A. Kumpan, S. J. Loucks, S. A. Letzring, F. J. Marshall, R. L. McCrory, S. F. B. Morse, W. Seka, J. M. Soures, and C. P. Verdon, Opt. Commun. **133**, 495 (1997).

13. S. Skupsky and R. S. Craxton, Phys. Plasmas **6**, 2157 (1999).

14. J. R. Rygg, J. A. Frenje, C. K. Li, F. H. Séguin, R. D. Petrasso, J. A. Delettrez, V. Yu. Glebov, V. N. Goncharov, D. D. Meyerhofer, S. P. Regan, T. C. Sangster, and C. Stoeckl, Phys. Plasmas **13**, 052702 (2006).

15. J. Delettrez, R. Epstein, M. C. Richardson, P. A. Jaanimagi, and B. L. Henke, Phys. Rev. A **36**, 3926 (1987).

16. F. H. Séguin, J. A. Frenje, C. K. Li, D. G. Hicks, S. Kurebayashi, J. R. Rygg, B.-E. Schwartz, R. D. Petrasso, S. Roberts, J. M. Soures, D. D. Meyerhofer, T. C. Sangster, J. P. Knauer, C. Sorce, V. Yu. Glebov, C. Stoeckl, T. W. Phillips, R. J. Leeper, K. Fletcher, and S. Padalino, Rev. Sci. Instrum. **74**, 975 (2003).

17. R. A. Lerche and T. J. Murphy, Rev. Sci. Instrum. **63**, 4880 (1992).

18. J. A. Frenje, C. K. Li, F. H. Séguin, J. Deciantis, S. Kurebayashi, J. R. Rygg, R. D. Petrasso, J. Delettrez, V. Yu. Glebov, C. Stoeckl, F. J. Marshall, D. D. Meyerhofer, T. C. Sangster, V. A. Smalyuk, and J. M. Soures, Phys. Plasmas **11**, 2798 (2004).